

SUPPLEMENTARY INFORMATION

Collective protection against the type VI secretion system in bacteria

Elisa T. Granato^{*1,2}, William P. J. Smith^{* 1,2,3}, Kevin R. Foster^{1,2}

^{*}Equal contribution

¹ Department of Biology, University of Oxford, Oxford, UK

² Department of Biochemistry, University of Oxford, Oxford, UK

³ Division of Genomics, Infection and Evolution, University of Manchester, UK

SUPPLEMENTARY FIGURES

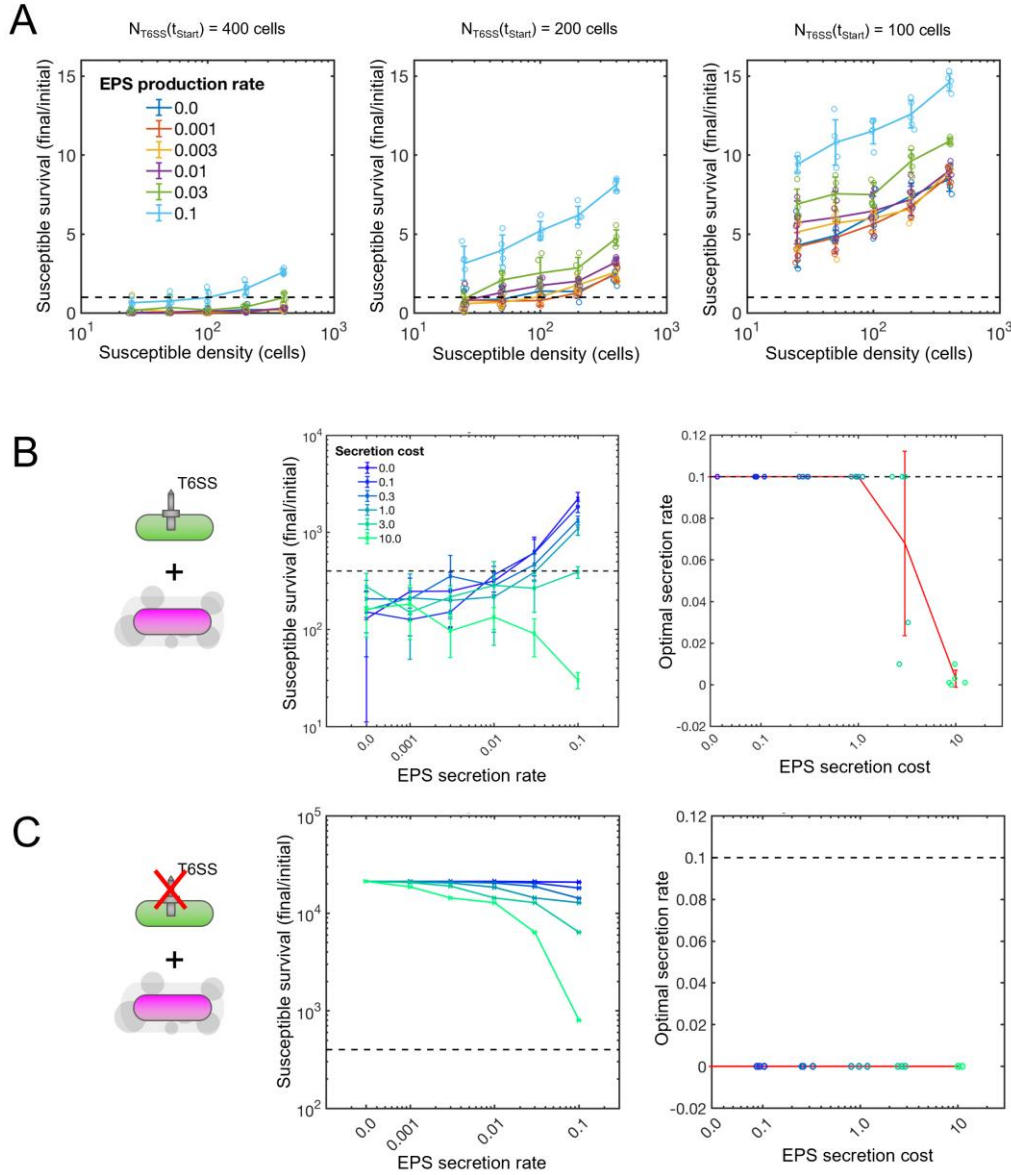
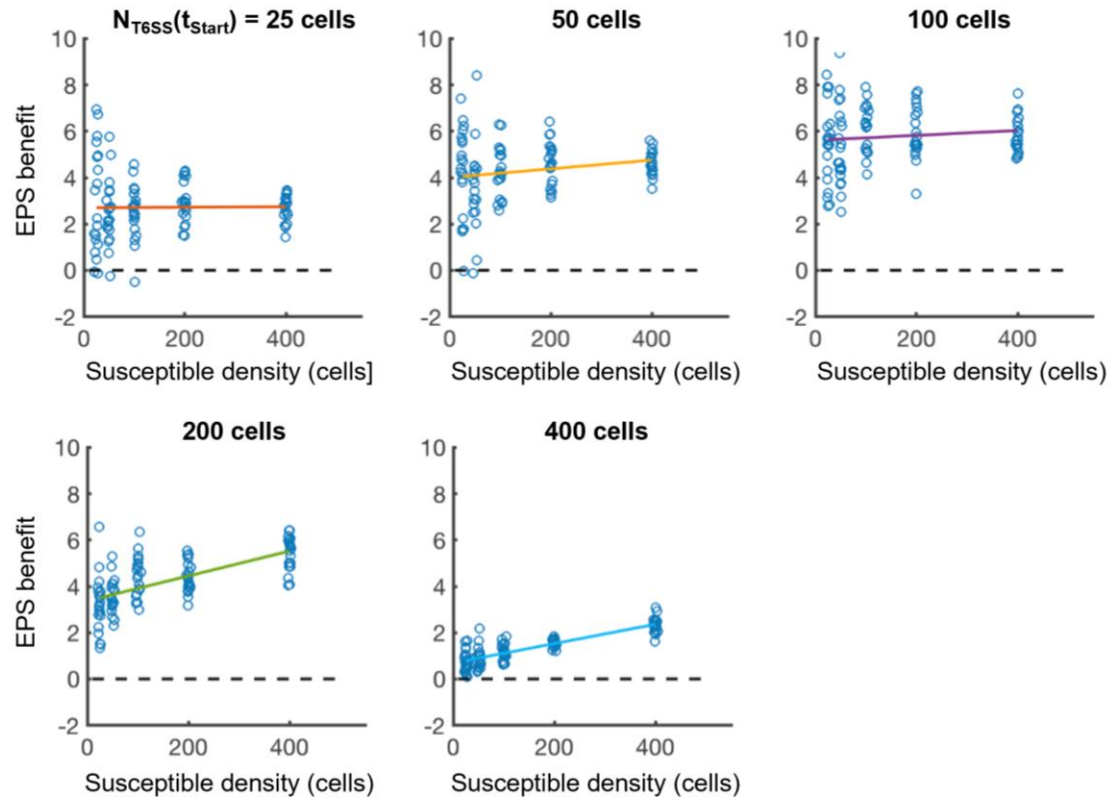


Fig. S1: The benefits of EPS protection vary with EPS secretion rate, cost and attacker density. (A) Measurements of final:initial susceptible cell counts as a function of initial susceptible cell density, for increasing EPS secretion rates P_{EPS} (see shared legend). From left to right, panels show data for three different starting attacker densities ($N_{T6SS}(t_{start}) = 400, 200$ and 100). Individual data points are shown; lines and error bars indicate data means and standard deviations, respectively. $N = 5$ simulation replicates per case. **(B)** Measurements of final:initial susceptible cell counts (left) against T6SS+ attackers ($k_{fire} = 200.0$ firings $cell^{-1} h^{-1}$), as a function of EPS secretion rate P_{EPS} , for increasing EPS cost values C_{EPS} (see legend). Each simulation begins with 400 attacker and 400 susceptible cells. Lines and error bars respectively show data means and standard deviations; $N = 5$ replicates per case. Right: plots of optimal secretion rate, showing the P_{EPS} values that maximised susceptible cell survival as a function of EPS cost C_{EPS} . Note that $P_{EPS} = 0.1$ is the maximum EPS secretion rate we allow, and so true optima may exceed those shown here. Data points are color-coded according to the legend shown in the left panel; red lines and bars indicate mean and standard deviation of measured optima. **(C)** Analogous to (B), except with susceptibles competing against a T6SS- attacker ($k_{fire} = 0.0$ firings $cell^{-1} h^{-1}$).

A



B

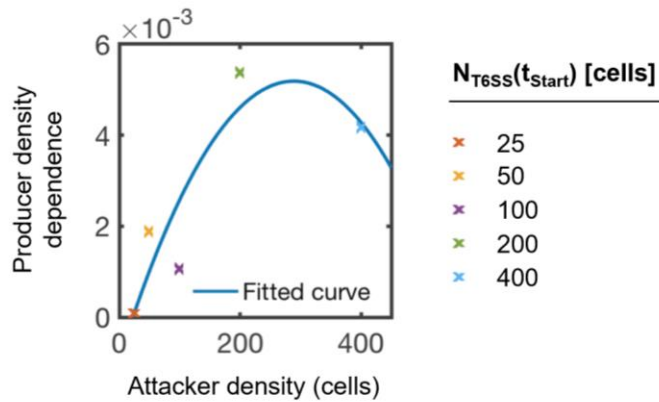


Fig. S2: EPS production often confers a density-dependent survival benefit against T6SS attacks. (A) Plots of EPS Benefit (see main text) against initial susceptible cell density for increasing initial attacker densities ($N_{T6SS}(t_{start})$ values indicated above panels). Individual data points shown alongside lines-of-best-fit, fitted using linear regression. Dashed lines correspond to EPS Benefit = 0. $N = 20$ simulation replicates per parameter combination. (B) Summary plot showing gradients of fitted lines in (A) ("Producer density dependence") as a function of attacker cell density. Individual data points are shown alongside a fitted quadratic curve (least-squares fitting, $R^2 = 0.5588$).

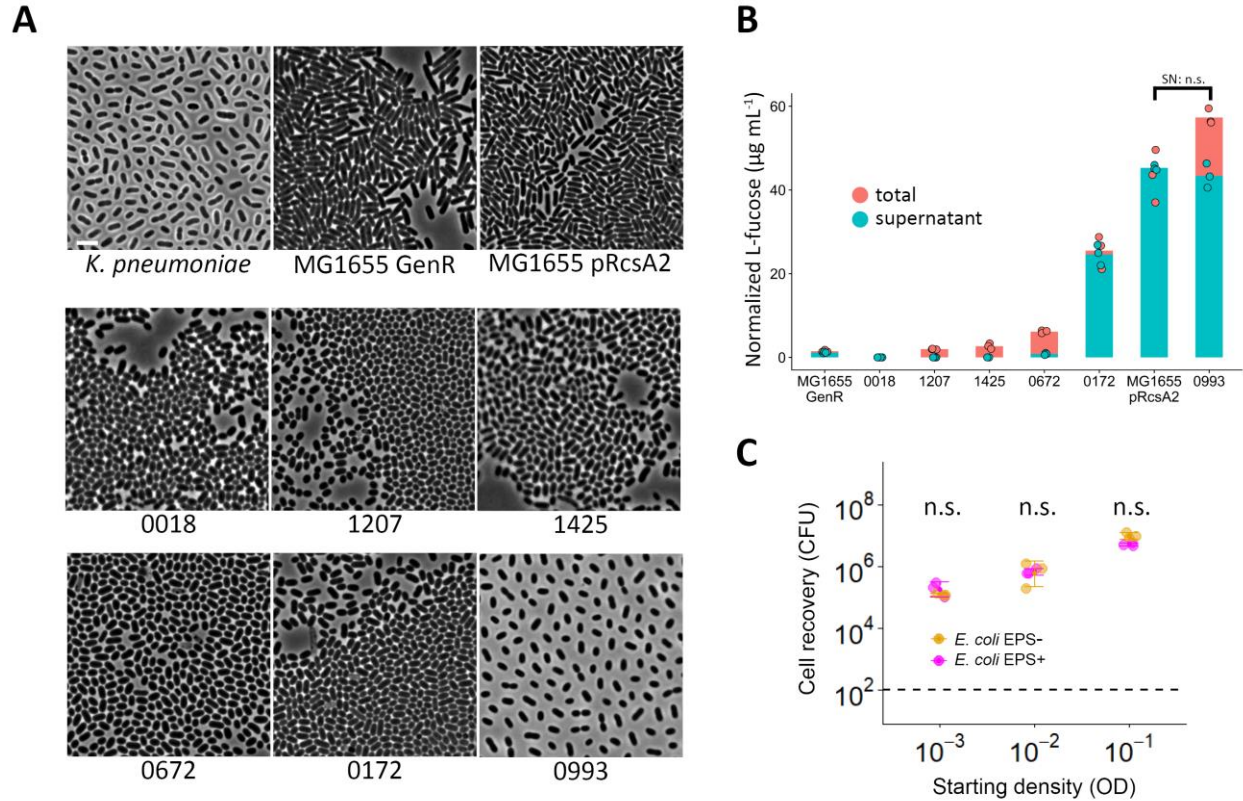


Fig. S3. EPS phenotype of engineered *E. coli* EPS-producing strain is comparable to that of clinical *E. coli* isolates and incurs no significant growth penalty. (A) Representative phase-contrast micrographs of EPS non-producing (MG1655 Gen^R) and EPS-producing (MG1655 pRcsA2) *E. coli* used in this study, as well as of several clinical *E. coli* isolates (see Table S2). Strains expressing membrane-bound capsules (e.g. isolate 0993) display large gaps between cells even if seeded at high densities. *Klebsiella pneumoniae* is shown as an example of a typical membrane-bound capsule phenotype. Scale bar, 5 μm . **(B)** To estimate relative colanic acid production, monocultures of different *E. coli* strains grown on plates were subjected to a spectrophotometric assay for L-fucose. Individual dots represent L-fucose concentrations normalized to optical density for total cell extracts (red) and supernatants (turquoise), respectively. Coloured bar plots represent mean values of three biological replicates. For each biological replicate, we measured both total cell extracts and supernatants. To test for differences in L-fucose concentration in supernatants (SN), we used a two-sided Wilcoxon rank sum test ($W = 6$, $p = 0.7$; n.s., not significant). **(C)** To test whether EPS production incurs a growth cost, EPS non-producing (MG1655 Gen^R; EPS-) and EPS-producing (MG1655 pRcsA2; EPS+) *E. coli* were competed against each other at 1:1 starting ratios. For each strain, cell recovery (CFU) after 6 h of co-culturing at different starting cell densities (optical density; OD) is shown. Individual data points ($n=3$) and their means are shown as larger dots and smaller dots, respectively. Error bars denote standard error of the mean. To test for differences in cell recovery, we used two-sided Wilcoxon rank sum tests (OD = 10^{-3} : $W = 6$, $p = 0.66$; OD = 10^{-2} : $W = 3.5$, $p = 0.82$; OD = 10^{-1} : $W = 6$, $p = 0.08$; n.s., not significant).

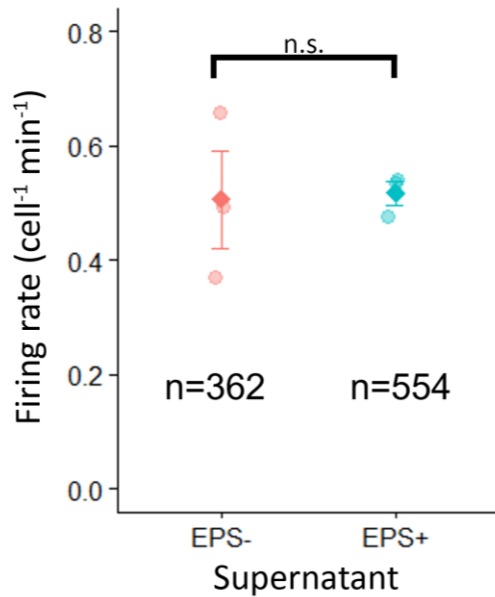
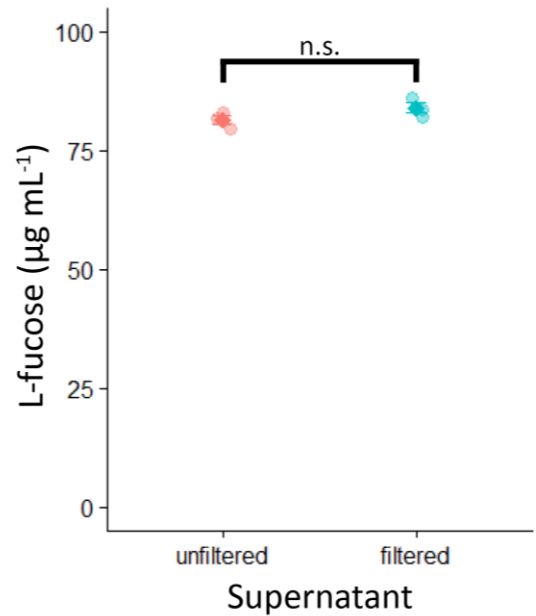
A**B**

Fig S4: T6SS firing rate is unaffected by the presence of exopolysaccharides. (A) T6SS firing rates in *A. baylyi* T6SS+ (*clpV-mcherry2*) exposed to cell-free supernatants of EPS- and EPS+ *E. coli*. Firing rates were determined by time-lapse microscopy and monitoring the appearance of fluorescent ClpV foci in focal cells over time. Darker shade dots represent mean values across three replicates. Error bars denote standard error of the mean. To test for differences in firing rate, we used a two-sided Wilcoxon rank sum test ($W = 4$, $p = 1$; n.s., not significant). n = total number of cells observed for each treatment. **(B)** To test whether sterile-filtering removes EPS from culture supernatants, filtered and unfiltered supernatants of MG1655 pRcsA2 monocultures ($n=3$) were subjected to a spectrophotometric assay for L-fucose. Individual dots represent L-fucose concentrations for either unfiltered supernatants, or supernatants filtered through a 0.2 μm filter. Darker shade dots represent mean values of three biological replicates. Error bars denote standard error of the mean. For each biological replicate, we measured both filtered and unfiltered supernatant. To test for differences in L-fucose concentration, we used a two-sided, paired samples Wilcoxon signed rank test ($V = 0$, $p = 0.25$; n.s., not significant).

SUPPLEMENTARY TABLES

Table S1. Model parameters used in this study

TYPE	Parameter	Symbol	Value(s)	Units	Source
T6SS attacks	T6SS firing rate	k_{fire}	200.0	firings cell ⁻¹ h ⁻¹	This study
	Lysis delay	$1 / k_{lysis}$	0.125	H	[1]
	Lethal hit threshold	N_{hits}	1, Infinity	-	Estimated from [2]
	Extracellular needle length	L_{needle}	0.5	microns	[1]
	Min. needle penetration	$L_{penetration}$	0.01	microns	[1]
Cells	Max. specific growth rate	k_{grow}	1.0	h ⁻¹	[3]
	Cell radius	R	0.5	microns	Estimated from [2]
	Cell volume at birth	V_0	1.16	microns ³	[4]
	Cell division volume noise	η_{div}	9	%	[4]
	Cell division orientation noise	η_{orient}	0.2	%	[4]
EPS	EPS particle radius	R_{EPS}	0.4	microns	This study
	EPS particle segment length	L_{EPS}	0.01	microns	This study
	EPS secretion probability per timestep	P_{EPS}	0.0-0.1	-	This study
	EPS secretion cost	C_{EPS}	0.0-10.0	-	This study
Numerical	Simulation timestep	Δt	0.025	h	[3]
	Cell / needle sorting grid size	h	10	microns	[1]
	Conjugate gradient absolute tolerance	e_{CG}	0.001	-	[3]
	Max. contact iterations	Max_{iter}	8	-	[3]
	Regularization weight	α	0.04	-	[4]
	Growth restriction factor	$1/\gamma$	0.002	-	[4]

Table S2. Strains and plasmids used in this study

STRAINS	Name	Species	Genotype	Isolation Site	Source
	T6SS+	<i>Acinetobacter baylyi</i>	ADP1 (vipA)-sfGFP; Str ^R	-	[1]
	T6SS-	<i>Acinetobacter baylyi</i>	ADP1 Δ tssM (vipA)-sfGFP; Str ^R	-	Marek Basler
	T6SS+ clpV-mCherry2	<i>Acinetobacter baylyi</i>	ADP1 (clpV)-mCherry2; Str ^R	-	Marek Basler
	MG1655	<i>Escherichia coli</i>	F- lambda- ilvG- rfb-50 rph-1	-	Colin Kleanthous
	EPS-	<i>Escherichia coli</i>	MG1655 Gen ^R	-	[5]
	EPS- (BFP)	<i>Escherichia coli</i>	MG1655 mTagBFP2::Tn7	-	This study
	EPS+	<i>Escherichia coli</i>	MG1655 pRcsA2; Amp ^R	-	This study
	EPS+ (mScarlet)	<i>Escherichia coli</i>	MG1655 mScarlet-I::Tn7 pRcsA2; Amp ^R	-	This study
	#0018	<i>Escherichia coli</i>	unsequenced clinical isolate #19Y000018	Urine	Nottingham Pathogen Bank
	#1207	<i>Escherichia coli</i>	unsequenced clinical isolate #17Y001207	Pus (Appendix)	Nottingham Pathogen Bank
	#1425	<i>Escherichia coli</i>	unsequenced clinical isolate #18Y001425	Fluid (Pancreas)	Nottingham Pathogen Bank
	#0672	<i>Escherichia coli</i>	unsequenced clinical isolate #17Y000672	Pus (Appendix)	Nottingham Pathogen Bank
	#0172	<i>Escherichia coli</i>	unsequenced clinical isolate #18Y000172	Urine	Nottingham Pathogen Bank
	#0993	<i>Escherichia coli</i>	unsequenced clinical isolate #18Y000993	Fluid (Pancreas)	Nottingham Pathogen Bank
	<i>K. pneumoniae</i>	<i>Klebsiella pneumoniae</i> subsp. <i>pneumoniae</i> DSM 30104	-	-	Frances Spragge

PLASMIDS	Name	Description	
	pGRG25- <i>Pmax::mScarlet-I</i>	pGRG25 vector for Tn7 integration [6], expressing mScarlet-I from the Pmax promoter [7]. Amp ^R	Thomas Meiller-Legrand
	pGRG25- <i>Pmax::mTagBFP2</i>	pGRG25 vector for Tn7 integration [6], expressing mTagBFP2 from the Pmax promoter [7]. Amp ^R	Thomas Meiller-Legrand
	pRcsA2	Encodes rcsA under the control of the lac promoter. Allows IPTG-inducible production of RcsA, which upregulates the expression of colanic acid synthesis genes from the chromosome. Amp ^R	[8]

Supplementary References

1. Smith WPJ, Vettiger A, Winter J, Ryser T, Comstock LE, Basler M, et al. The evolution of the type VI secretion system as a disintegration weapon. *PLOS Biol* 2020; **18**: e3000720.
2. Ringel PD, Hu D, Basler M. The role of type VI secretion system effectors in target cell lysis and subsequent horizontal gene transfer. *Cell Rep* 2017; **21**: 3927–3940.
3. Rudge TJ, Steiner PJ, Phillips A, Haseloff J. Computational modeling of synthetic microbial biofilms. *ACS Synth Biol* 2012; **1**: 345–352.
4. Smith WPJ, Davit Y, Osborne JM, Kim W, Foster KR, Pitt-Francis JM. Cell morphology drives spatial patterning in microbial communities. *Proc Natl Acad Sci U S A* 2017; **114**: E280–E286.
5. Basler M, Ho BT, Mekalanos JJ. Tit-for-tat: Type VI secretion system counterattack during bacterial cell-cell interactions. *Cell* 2013; **152**: 884–894.
6. McKenzie GJ, Craig NL. Fast, easy and efficient: site-specific insertion of transgenes into enterobacterial chromosomes using Tn7 without need for selection of the insertion event. *BMC Microbiol* 2006; **6**: 39.
7. Mavridou DAI, Gonzalez D, Clements A, Foster KR. The pUltra plasmid series: A robust and flexible tool for fluorescent labeling of Enterobacteria. *Plasmid* 2016; **87–88**: 65–71.
8. Joshi N, Ngwenya BT, French CE. Enhanced resistance to nanoparticle toxicity is conferred by overproduction of extracellular polymeric substances. *J Hazard Mater* 2012; **241–242**: 363–370.